

Excitation of nonlinear electron acoustic waves

Francesco Valentini

*Dipartimento di Fisica and INFM, Università della Calabria, 87036 Rende (CS) Italy,
and Department of Physics, University of California at San Diego, La Jolla, California, 92093*

Thomas M. O'Neil and Daniel H. E. Dubin

Department of Physics, University of California at San Diego, La Jolla, California, 92093

(Received 12 June 2005; accepted 31 March 2006; published online 10 May 2006)

A particle in cell (PIC) simulation is used to investigate the excitation of electron acoustic waves (EAWs) and the stability of the EAWs against decay. An EAW is a nonlinear wave with a carefully tailored trapped particle population, and the excitation process must create the trapped particle population. For a collisionless plasma, successful excitation occurs when a relatively low amplitude driver that is spatially and temporally resonant with the EAW is applied for a sufficiently long time (many trapping periods). The excited EAW rings at a nearly constant amplitude long after the driver is turned off, provided the EAW has the largest wavelength that fits in the simulation domain. Otherwise, the excited EAW decays to a longer wavelength EAW. In phase space, this decay to longer wavelength appears as a tendency of the vortex-like trapped particle populations to merge. In a collisional plasma, successful excitation of an EAW requires the driver amplitude to exceed a threshold value. The period for a trapped particle oscillation must be short compared to the time for collisions to smooth out the trapped particle plateau. © 2006 American Institute of Physics. [DOI: 10.1063/1.2198467]

I. INTRODUCTION

In 1991, Hollway and Dorning¹ noted that certain nonlinear wave structures can exist in a plasma, even at low amplitude. They called these waves electron-acoustic waves (EAW) since the dispersion relation is of the acoustic form (i.e., $\omega = 1.31kv_{th}$ for small k). Here, ω is the angular frequency of the wave, k the wavenumber, and v_{th} the thermal velocity of the plasma electrons.

Note that EAWs are quite distinct from ion-acoustic waves, which are linear waves that involve both electrons and ions. The EAWs are higher frequency nonlinear waves that involve only the electrons; the ions simply provide a uniform neutralizing background charge.

Within linear theory, an EAW would be heavily Landau damped, since the wave phase velocity is comparable to the electron thermal velocity.² However, the EAW is a Bernstein-Green-Kruskal nonlinear mode (BGK mode)³ with electrons trapped in the wave troughs. Because of the trapped electrons, the distribution of electron velocities is effectively flat at the wave phase velocity, and this turns off Landau damping.

These waves can be constructed even at low amplitude by carefully tailoring the trapped particle distribution. However, the importance of the waves as elementary excitations of the plasma (such as Langmuir waves) depends on the extent to which they are excited by general perturbations and drives applied to the plasma, and the extent to which they are stable against decay to other modes. Because EAWs are intrinsically nonlinear structures, one expects that parametric decay instabilities are possible.

A simple argument shows that the waves can be excited by a sudden (or initial) perturbation only at large amplitude. We assume here that the trapped particle distribution does

not exist initially, but forms dynamically as the wave evolves. For a wave electric field $E \sin(kx - \omega t)$, the time to form the trapped particle distribution is approximately the period for trapped particles to oscillate in the trough of the wave, $\tau_{trap} = 2\pi\sqrt{m/(eEk)}$, where e and m are the electron charge and mass, respectively.⁴ The wave is killed by Landau damping before the trapped particle distribution can form unless $\gamma_L \tau_{trap} < 1$, where γ_L is the linear Landau damping rate.² For a wave with phase velocity comparable to the thermal velocity ($\omega/k \sim v_{th}$), the Landau damping rate is comparable to the frequency ($\gamma_L \sim kv_{th}$), so the initial amplitude must be large (i.e., $e\phi \sim eE/k \sim mv_{th}^2 = T_e$).

However, we will see that EAWs can be launched by a small amplitude driver if the driver is applied resonantly over many trapping periods. The driver continuously replenishes the energy removed by Landau damping, so the trapped particle distribution (and the EAW) is eventually produced. This result will be demonstrated using a particle in cell (PIC) simulation.^{5,6} For the case where the wavelength is the longest wavelength that fits in the plasma and the plasma is collisionless, the launched EAW persists at nearly constant amplitude long after the driver is turned off. For the large number of particles used in the PIC simulation ($N \approx 5 \times 10^6 - 10^7$), the effect of collisions is negligible over the duration of the run.

When Coulomb collisions are explicitly added to the simulation, there is a threshold for a driver amplitude that is large enough to launch an EAW. The threshold is due to a competition between trapping and collisional effects. Trapping oscillations try to make the distribution flat at the wave phase velocity (create a plateau), whereas collisions try to maintain the Maxwellian velocity distribution. The driver amplitude must be sufficiently large that the trapping period,

$\tau_{\text{trap}} = 2\pi/\sqrt{ekE/m}$, is smaller than the time for collisions to smooth out the plateau.

Finally, stability of the EAWs against decay to other modes is investigated. As mentioned, an EAW with wavelength equal to the length of the plasma can be resonantly launched by a low amplitude driver and then persists at a nearly constant amplitude long after the driver is turned off. Here, collisional damping is negligible in the simulation. When this EAW is replicated in space and used as an initial condition for the simulation of a much longer plasma, the EAW is observed to decay to longer wavelength EAWs. In phase space, the trapped particles for an EAW appear to be a vortex structure, and the decay to a longer wavelength involves a merger of the vortices.⁷⁻¹¹

Our results are complementary to recent results reported by Afeyan, Won, Savchenko, Johnson, Ghizzo, and Bertrand.¹² These authors also carry out numerical simulations of nonlinear waves launched by a driver in an unmagnetized plasma. Motivated by suggestions that EAWs might be launched in laser-plasma interaction experiments,¹³ Afeyan *et al.* focused on relatively large driver amplitudes. They found novel BGK waves that they call “Kinetic Electrostatic Electron Nonlinear (KEEN) Waves.” These waves are comprised of four or five significant phase-locked harmonics, persist only when driven hard enough, and are driven by a wide range of frequencies. In contrast to our work, these authors reported that low amplitude drive does *not* produce coherent EAWs, presumably because the driver was not applied resonantly for a long enough time. We will see that the resonance is relatively narrow and can easily be missed.

II. DISPERSION RELATIONS

For convenience, we scale time by the inverse plasma frequency ω_p^{-1} , where $\omega_p = \sqrt{4\pi ne^2/m}$ and n is the electron density. The length is scaled by the Debye length $\lambda_D = v_{\text{th}}/\omega_p$. With these choices, velocity is scaled by the electron thermal velocity $\lambda_D \omega_p = v_{\text{th}}$ and electric field by $\sqrt{4\pi nmv_{\text{th}}^2}$.

Using these scalings, the Landau dispersion relation takes the form²

$$1 - \frac{1}{k^2} \int_L dv \frac{\partial f_0 / \partial v}{v - \omega/k} = 0, \quad (1)$$

where $\omega = \omega_r - i\gamma$ is the complex frequency, k the wavenumber, and $f_0(v)$ the distribution of electron velocity components in the direction of wave propagation. Here, we take this distribution to be Maxwellian, $f_0(v) = \exp(-v^2/2)/\sqrt{2\pi}$. The subscript L on the integral sign indicates that the velocity integral is to be taken along the Landau contour, dropping down around the pole at $v = \omega/k$. For the high frequency modes of interest, the ions do not participate; throughout the paper the ions are taken to be a uniform neutralizing background charge.

For the case where the phase velocity is large compared to the thermal velocity ($v_\phi \equiv \omega/k \gg 1$), Eq. (1) yields the weakly damped dispersion root, $\omega = (1 + 3k^2)^{1/2}$ and $\gamma = \gamma_L =$

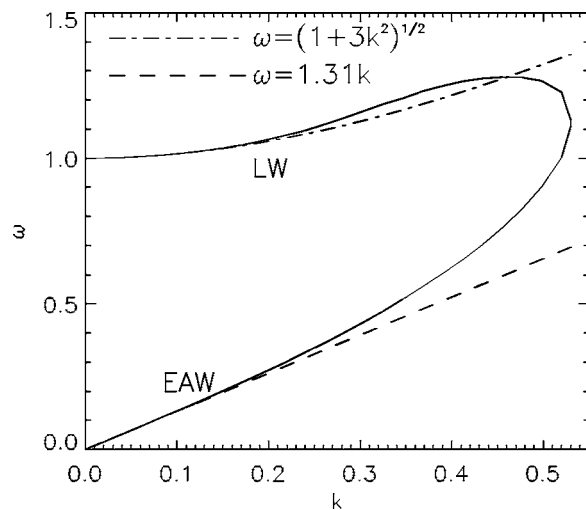


FIG. 1. The “thumb” dispersion relation. The frequency is expressed in units of the electron plasma frequency and the wavenumber in units of the inverse of the electron Debye length.

$-\sqrt{\pi/2}(v_\phi^2/k)e^{-v_\phi^2/2}$. This is Landau’s well-known solution for the frequency and damping rate of a Langmuir wave (LW). Since the phase velocity is large compared to the thermal velocity, the damping rate is exponentially small.

There are other more heavily damped roots for smaller phase velocity. For example, there is a root at $\omega_r \approx 3.6k$ and $\gamma \approx k$,^{14,15} which can be thought of as the linear progenitor of the EAW.

For sufficiently weak damping, the velocity integral along the Landau contour can be approximated by

$$\int_L dv \frac{\partial f_0 / \partial v}{v - \omega/k} = P \int_{-\infty}^{+\infty} dv \frac{\partial f_0 / \partial v}{v - \omega/k} + \pi i \left. \frac{\partial f_0}{\partial v} \right|_{\omega/k}, \quad (2)$$

where P indicates that the principle part is to be taken. As mentioned earlier, the trapped particle distribution for an EAW effectively makes the distribution flat at the wave phase velocity (i.e., $\partial f_0 / \partial v|_{\omega/k} \approx 0$). Thus, Holloway and Dorning¹ obtain a dispersion relation for small amplitude EAWs by retaining only the principle part in the velocity integral of Eq. (1).

Solving for the roots of the resulting dispersion relation then yields the solid curve in Fig. 1. This so-called “thumb” dispersion curve exhibits two roots for small k . The upper root [$\omega = (1 + 3k^2)^{1/2}$] is the LW and the lower root ($\omega = 1.31k$) is the EAW.

We emphasize that Fig. 1 describes only small amplitude EAWs. Using a Maxwellian distribution for $f_0(v)$ and taking the principle value in the velocity integral assumes that the width of the plateau, where $\partial f_0 / \partial v = 0$, is infinitesimal. For a finite amplitude EAW, the plateau width is the velocity range over which electrons are trapped in the wave troughs, that is Δv_{trap} , where $(\Delta v_{\text{trap}})^2 \sim E/k$. An infinitesimal trapping width corresponds to an infinitesimal wave amplitude. We will see that the phase velocity for a large amplitude EAW is shifted upward from the value indicated in Fig. 1.

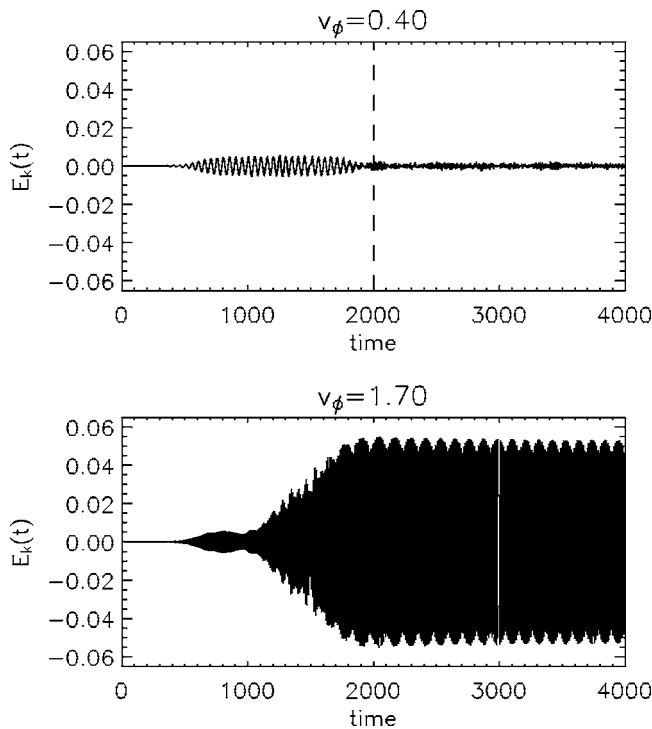


FIG. 2. Plasma response for two different values of the driver phase velocity: $v_\phi=0.4$ (at the top) and $v_\phi=1.70$ (at the bottom).

III. PARTICLE IN CELL SIMULATIONS

A. Excitation of the EAWs

The PIC simulation follows the electron dynamics in the x direction, which is the direction of wave propagation. The electron phase space domain for the simulation is $D = [0, L_x] \times [-v_{\max}, v_{\max}]$, where $v_{\max}=5$. For an initial set of simulations, we choose $L_x=2\pi/k=20$, but in later simulations the plasma length is increased to $L_x=40$ and $L_x=80$. This increase in length allows for decay to longer wavelength EAWs. The time step is $\Delta t=0.1$. The simulations follow the evolution of $N \sim 5 \times 10^6$ to 10^7 electrons for many plasma periods ($t_{\max}=4000$). The initial electron velocity distribution is taken to be Maxwellian. Periodic boundary conditions in physical space are imposed, and Poisson's equation

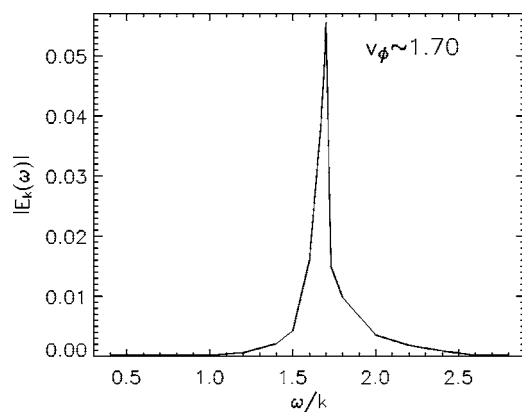


FIG. 3. The peak of resonance for the EAW.

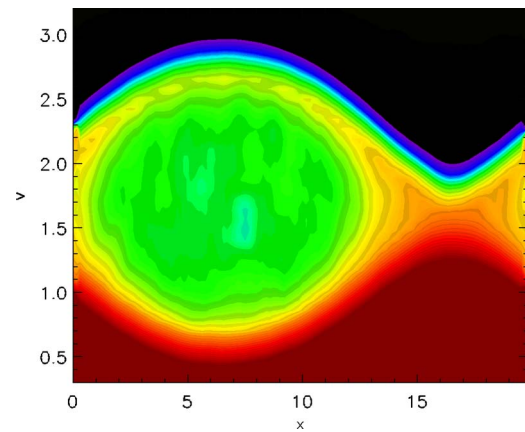


FIG. 4. (Color online) The phase space contour plot of the distribution function f at $t=4000$.

is solved using a standard Fast Fourier Transform (FFT) routine. The external driver electric field is taken to be of the form

$$E_D(x,t) = E_D^{\max} \left[1 + \left(\frac{t-\tau}{\Delta\tau} \right)^n \right]^{-1} \sin(kx - \omega t), \quad (3)$$

where $E_D^{\max}=0.01$, $\tau=1200$, $\Delta\tau=600$, $n=10$, and $k=\pi/10$. The plasma response is studied as a function of the driver frequency ω , or, equivalently, phase velocity $v_\phi=\omega/k=10\omega/\pi$. An abrupt turn on (or off) of the driver field would excite LWs as well as EAWs, complicating the analysis. Thus, the driver is turned on and off adiabatically. The driver amplitude is near E_D^{\max} (within a factor of 2) for several trapping periods ($t_{\text{off}}-t_{\text{on}} \approx 1200 \approx 11\tau_{\text{trap}}$), and is near zero again by $t_{\text{off}}=2000$. Here, the trapping period associated with the maximum driver field is $\tau_{\text{trap}}=2\pi/\sqrt{kE_D^{\max}}=112$.

Figure 2 shows the evolution of the plasma electric field, $E_k(t)$, for two different values of the driver phase velocity. In the top graph (for $v_\phi=0.4$), $E_k(t)$ rises to a small value while the driver is on, but falls to zero when the driver is turned off. The time t_{off} is indicated by the dashed line. In the bot-

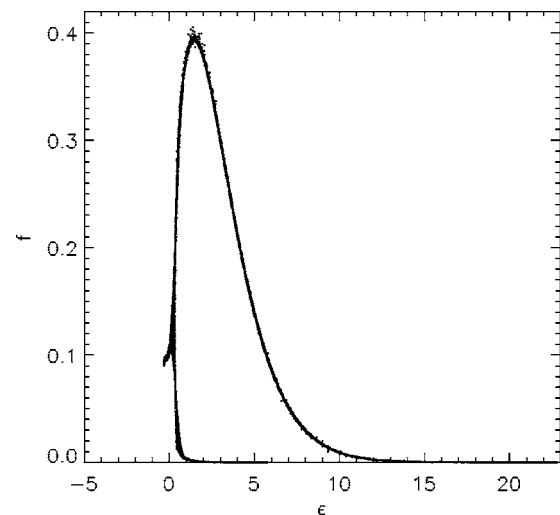


FIG. 5. Scatter plot of the distribution function f as a function of the energy in the wave frame $\epsilon=(v-v_\phi)^2/2-\phi(x,t_{\max})$.

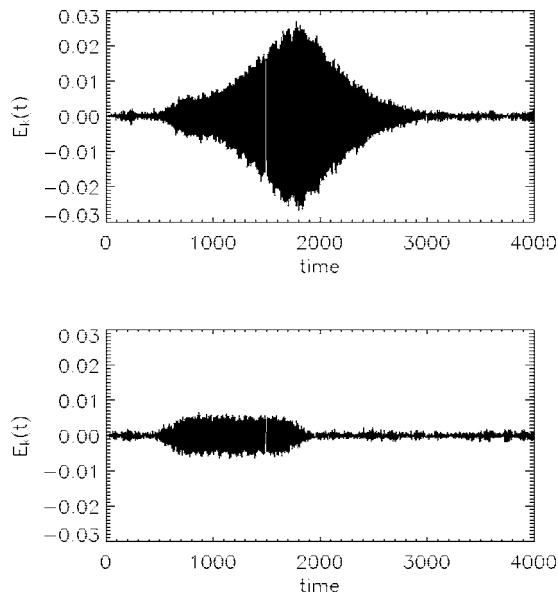


FIG. 6. Time evolution of the spectral component of the electric field, plotted for different values of the parameter r and for $v_\phi = 1.70$.

tom graph (for $v_\phi = 1.70$), $E_k(t)$ grows to large amplitude and maintains this amplitude (rings) after the driver is turned off.

Repeating such simulations for many different phase velocities (but holding the other driver parameters fixed at the values listed) yields the peaked graph in Fig. 3. Here, the

ordinate is the amplitude of the oscillating plasma electric field at the end of the simulation (long after the driver has been turned off), and the abscissa is the driver phase velocity. For this set of driver parameters, an EAW is driven resonantly for phase velocity $v_\phi \approx 1.70$.

For the wavenumber $k = \pi/10$, Figure 1 implies the resonant phase velocity $v_\phi \approx 1.45$. However, we must remember that Fig. 1 applies only to small amplitude (infinitesimal) EAWs. For the relatively large EAW in the simulation, the resonant phase velocity is shifted up to 1.70 by the finite plateau width. A separate calculation, for which dispersion relation (2) is solved numerically for the distribution function $f(v) = f_M(v) - [f_M(v) - f_M(v_\phi)] \{1 + [2(v - v_\phi)/\Delta v_{\text{trap}}]^{20}\}^{-1}$ (where f_M indicates a Maxwellian function), yields the phase velocity $v_\phi \approx 1.74$. In this distribution, the plateau width is taken to be the trapping width $\Delta v_{\text{trap}} = 2\sqrt{2E_k^{\text{sat}}/k}$, for the saturated amplitude $E_k^{\text{sat}} = 2E_k^{\text{sat}} \approx 0.11$.

As a more accurate procedure, we show that the distribution function obtained in the simulation is a BKG structure and use the BGK formalism to get the EAW solution. Figure 4 shows a false color contour plot of the electron distribution, $f(x, v)$, at the end of the run ($t_{\text{max}} = 4000$). The color code assigns higher values of f to longer wavelengths in the spectrum. The vortex-like structure in Fig. 4 represents trapped particles, and, as expected, these particles have a mean velocity equal to the phase velocity $v = 1.7$. The velocity width of the trapped particle region is about $\Delta v_{\text{trap}} \approx 1.7$,

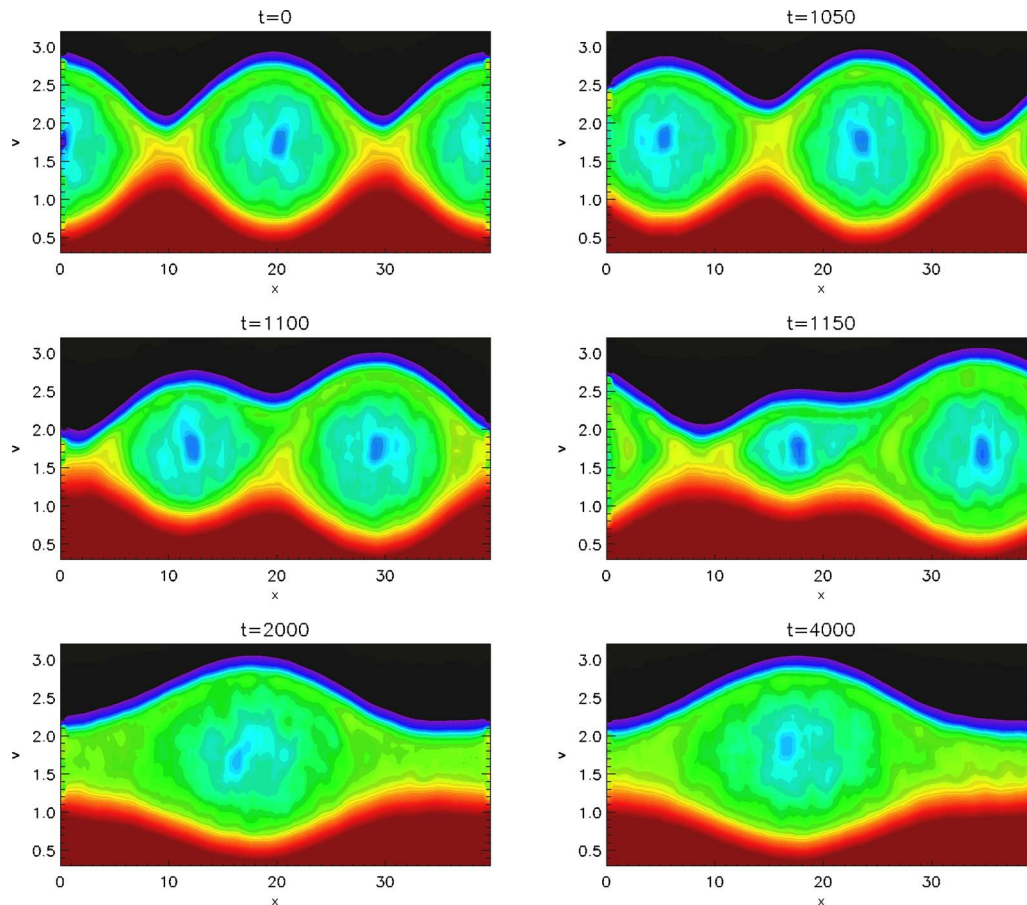


FIG. 7. (Color online) The coalescence and merging of two phase space holes.

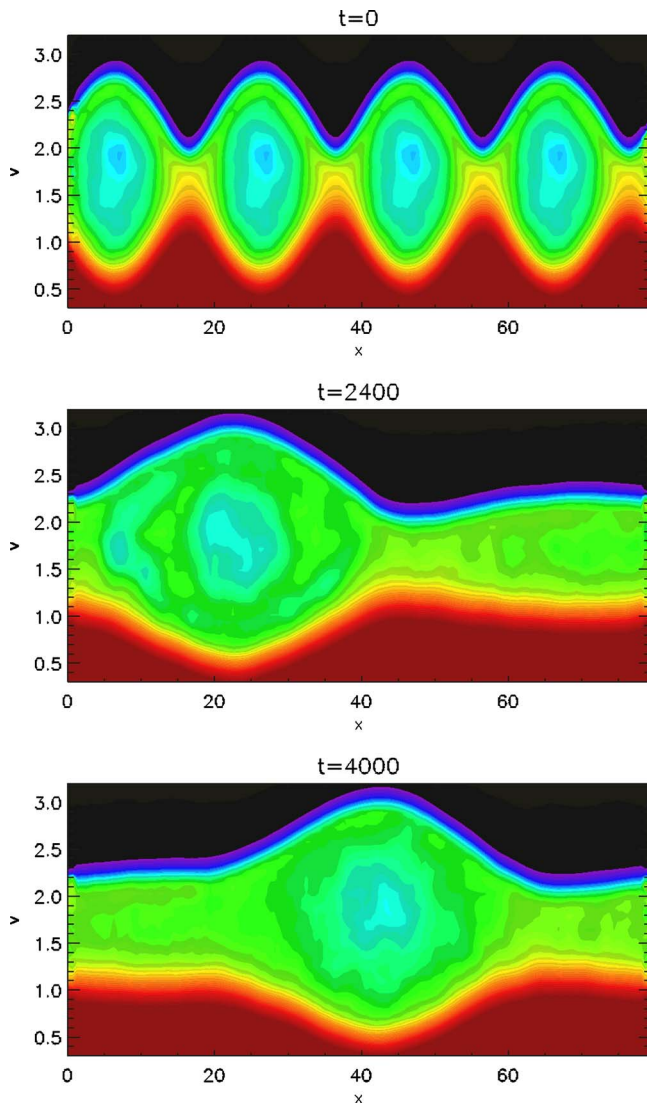


FIG. 8. (Color online) The coalescence and merging of four phase space holes.

which is in agreement with the theoretical expectation $\Delta v_{\text{trap}} = 2\sqrt{2E_k^{\text{sat}}/k} = 1.674$. Here, the saturation amplitude of the electric field is $E^{\text{sat}} = 2E_k^{\text{sat}} \approx 0.11$ (see the bottom graph in Fig. 2). In Fig. 5, we plot the distribution function f at the end of the run as a function of the energy in the wave frame $\epsilon = (v - v_\phi)^2/2 - \phi(x, t_{\text{max}})$. That is, for each (x, v) in the simulation domain, we plot $f(x, v)$ vs $\epsilon(x, v)$, resulting in the single curve shown in Fig. 5. The fact that the points in this scatter plot fall on a single curve shows that the electron distribution f is a function of the energy ϵ alone, as expected for a BGK distribution. By using this distribution in the BGK formalism³ for the phase velocity $v_\phi = 1.7$ and the electric potential amplitude $E^{\text{sat}}/k \approx 0.35$, we get a sinusoidal solution whose wavelength is $\lambda_{\text{BGK}} \approx 19.5$, which is very close to the wavelength of the electric perturbation in the simulation ($\lambda = 20$).

B. Effect of collisions

For a PIC simulation with one spatial dimension and with grid spacing smaller than the Debye length ($\Delta x/\lambda_D$

$\approx 1/6$ in our simulations), the effective collision time is longer than $t = \omega_p^{-1} n \lambda_D$, where $n = N/L_x$ is the one-dimensional (1-D) density of particles in the simulation.⁵ In scaled units, the collision time is larger than $t = N/L_x \approx 5 \times 10^5$ (for $L_x = 20\lambda_D$), which is much longer than duration of our runs $t_{\text{max}} = 4000$. This estimate is consistent with the empirical observation that the EAW in Fig. 2 persists at a nearly constant amplitude after the driver is turned off. To determine the effect of collisions on the EAW lurching process, we explicitly add collisions to the simulation using a Langevin model. The equation of motion for each electron is taken to be

$$\frac{dv}{dt} = E(x, t) + R(t) - \nu v, \quad (4)$$

where $-\nu v$ is the collisional drag, ν is the collision frequency, and $R(t)$ the stochastic acceleration. Each time step, Δt , the stochastic acceleration term provides a velocity step δv of random sign. This step produces velocity diffusion with diffusion coefficient $D_v = (\delta v)^2/2 \Delta t$. According to the Einstein relation, the collision frequency and diffusion coefficient are related through $\nu = D_v$. (Recall that $v_{\text{th}}^2 = 1$ in scaled units.)

As mentioned earlier, collisions introduce a competition between the effort of trapping to produce a plateau and the effort of velocity diffusion to smooth out the plateau. An estimate of the time for collisional velocity diffusion to smooth out a plateau of width Δv is $\tau_{\text{diff}} \approx (\Delta v)^2/2D_v = (\Delta v)^2/2\nu$. For small $\Delta v/v_{\text{th}}$, this time is much smaller than ν^{-1} ; physically, the time for a small angle scattering ($\delta\theta \approx \Delta v/v_{\text{th}}$) is much smaller than the time for an effective 90° scattering. For a plateau width corresponding to trapping in the driver field [i.e., $(\Delta v)^2/4 = E_D^{\text{max}}/k$], the time to smooth out the plateau is $\tau_{\text{diff}} \approx 2E_D^{\text{max}}/(k\nu)$. As a measure of the competition between trapping and collisional smoothing we introduce the time scale ratio

$$r = \frac{\tau_{\text{diff}}}{\tau_{\text{trap}}} = \frac{(E_D^{\text{max}})^{3/2}}{\pi \nu k^{1/2}}, \quad (5)$$

where $\tau_{\text{trap}} = 2\pi/\sqrt{kE_D^{\text{max}}}$ is the trapping period for the maximum driver amplitude.

We consider the evolution of the plasma electric field for three values of the parameter r . In each case the driver electric field is as specified earlier and the phase velocity is the resonant value $v_\phi = 1.7$. The case of negligibly weak collisionality (i.e., $r \gg 1$) is the bottom graph in Fig. 2. A case of intermediate collisionality ($r \approx 9.3$) is the top graph in Fig. 6. For this case, the plasma electric field is driven resonantly to large amplitude while the driver is on, but then damps away when the driver is turned off. A case of stronger collisionality ($r \approx 1.14$) is shown as the bottom graph in Fig. 6. Here, the plasma electric field remains small, since collisions effectively preclude the formation of a trapped particle plateau. We conclude that the condition $r > 1$ specifies a threshold for the launching of EAWs.

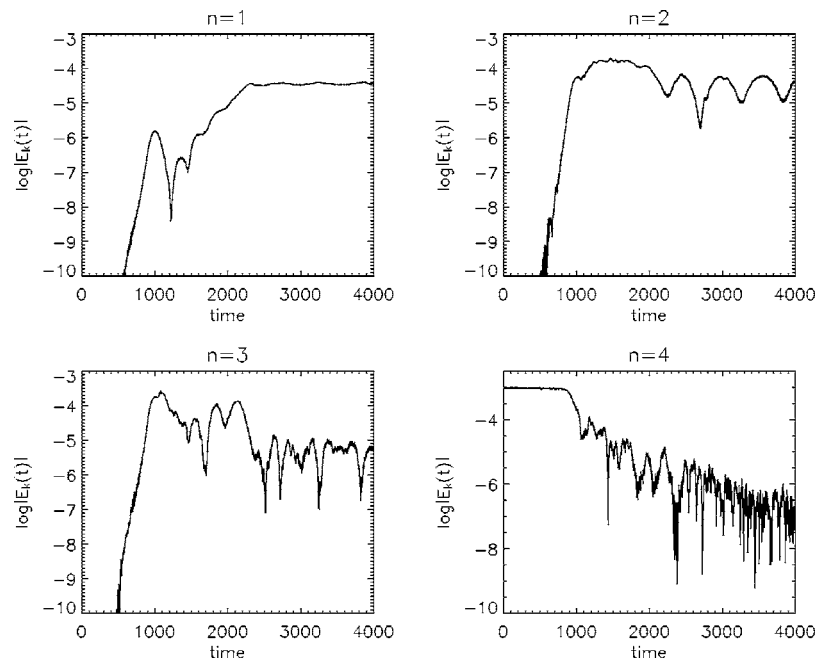


FIG. 9. Time evolution of the electric field spectral components $n=1, 2, 3, 4$. The fundamental mode $n=4$ decays at $t \approx 1000$.

C. Decay instability

Returning again to the case where the plasma is collisionless, we note again that the EAW in the bottom graph of Fig. 2 rings at nearly constant amplitude after the driver is turned off. However, the wavelength for this mode is the longest wavelength that fits in the simulation domain, so the constant amplitude is no guarantee against decay to a longer wavelength mode. Moreover, previous theory suggested that BGK modes with trapped particles may be subject to such decay instabilities.⁷⁻¹¹

To investigate the possibility of decay to a longer wavelength mode, we replicate the mode periodically in space and use it as the initial condition for a simulation in a longer domain. The matching from wavelength to wavelength is smooth since periodic boundary conditions were used in the initial simulation.

Figure 7 shows a temporal sequence of phase space contours for the case where the simulation domain has been doubled in length ($L_x=20 \rightarrow L_x=40$). The contour plot for $t=0$ is simply two copies of the plot in Fig. 4 placed side by side. The $t=0$ plot shows two vortex-like structures representing trapped particles. The sequence of plots shows a progressive merger of the two vortices until there is only a single vortex at $t=4000$. A decay instability has transferred the energy from mode 2 (i.e., $k=2 \cdot 2\pi/40=\pi/10$), to mode 1 (i.e., $k=1 \cdot 2\pi/40=\pi/20$); that is, to the longest wavelength that fits in the simulation domain.

Also, we have carried out simulations for $L_x=80$ (four initial vortices) and again observed merger to a single vortex. Figure 8 shows phase space contour plots for the times $t=0, 2400$, and 4000 , and Fig. 9 shows the time evolution of the electric field for the modes $n=1, 2, 3$, and 4 . Initially, mode 4 [i.e., $k=4 \cdot (2\pi/80)=\pi/10$] is excited, but begins to decay at $t=1000$. By $t=2400$, mode 1 has reached a constant amplitude, and merger to a single vortex has taken place. However, even at the end of the run ($t=4000$), there is significant energy content in modes 2 and 3, since the wave structure is distorted from sinusoidal.

From these observations, we expect that merger to a single vortex (or decay to the longest mode) is a general tendency for EAWs. This would be consistent with observations for the merger of phase space vortices in other situations, such as the vortical holes that result from the two stream instability.⁷⁻¹¹

From these observations, we expect that merger to a single vortex (or decay to the longest mode) is a general tendency for EAWs. This would be consistent with observations for the merger of phase space vortices in other situations, such as the vortical holes that result from the two stream instability.⁷⁻¹¹

ACKNOWLEDGMENTS

The authors gratefully acknowledge useful discussions with J. J. Dornig. This work was supported by the Fondazione Angelo Della Riccia, Firenze (Italy), the Center of Excellence for High Performance Computing, Cosenza (Italy), and National Science Foundation Grant No. PHY0354979.

¹J. P. Holloway and J. J. Dornig, Phys. Rev. A **44**, 3856 (1991).

²L. D. Landau, J. Phys. (Moscow) **10**, 25 (1946).

³I. B. Bernstein, J. M. Green, and M. D. Kruskal, Phys. Rev. **108**, 546 (1957).

⁴T. O'Neil, Phys. Fluids **8**, 2255 (1965).

⁵C. K. Birdsall and A. B. Langdon, *Plasma Physics Via Computer Simulation* (McGraw-Hill, Singapore, 1985), Chap. 3 and Chap. 12, p. 274.

⁶D. H. Dubin, *Numerical and Analytical Methods For Scientists and Engineers Using MATHEMATICA* (Wiley-Interscience, Hoboken, NJ, 2003), Sec. 7.3 (electronic version only).

⁷H. L. Berk, C. E. Nielsen, and K. V. Roberts, Phys. Fluids **13**, 980 (1970).

⁸A. Ghizzo, B. Izrar, P. Bertrand, E. Fijalkov, M. R. Feix, and M. Shoucri, Phys. Fluids **31**, 72 (1988).

⁹G. Manfredi and P. Bertrand, Phys. Plasmas **7**, 2425 (2000).

¹⁰D. C. DePackh, J. Electron. Control **13**, 417 (1962).

¹¹R. A. Dory, J. Nucl. Energy, Part C **6**, 511 (1964).

¹²B. Afeyan, K. Won, V. Savchenko, T. W. Johnston, A. Ghizzo, and P. Bertrand, "Kinetic electrostatic electron nonlinear (KEEN) waves and their interactions driven by the ponderomotive force of crossing laser beams," *IFSA Proceedings, 2003*, edited by B. A. Hammel, D. D. Meyer-

hofer, J. Meyer-ter-Vehn, and H. Azechi (American Nuclear Society, Inc., La Grange Park, IL, 2004), Chap. V, pp. 213–217.

¹³D. S. Montgomery, R. J. Focia, H. A. Rose, D. A. Russell, J. A. Cobble, J. C. Fernandez, and R. P. Johnson, Phys. Rev. Lett. **87**, 155001 (2001).

¹⁴B. D. Fried and R. W. Gould, Phys. Fluids **4**, 139 (1961).

¹⁵D. C. Montgomery, *Theory of Unmagnetized Plasmas* (Gordon and Breach, New York, 1962), p. 218.